Energy 164 (2018) 264–274

Contents lists available at ScienceDirect

Energy

journal homepage: www.elsevier.com/locate/energy

Response surface study and kinetic modelling of biodiesel synthesis catalyzed by zinc stearate

Mariana S. Alvarez Serafini [b], Deborath M. Reinoso [a, b], Gabriela M. Tonetto [a, b, *]

[a] Departamento de Ingeniería Química, Universidad Nacional del Sur (UNS), Argentina
[b] Planta Piloto de Ingeniería Química – PLAPIQUI (UNS-CONICET), Camino La Carrindanga km 7, 8000 Bahía Blanca, Argentina

ARTICLE INFO

Article history:
Received 9 November 2017
Received in revised form
13 August 2018
Accepted 24 August 2018
Available online 25 August 2018

Keywords:
Transesterification
Fatty acid methyl esters
Zinc stearate
Kinetic model

ABSTRACT

This contribution reports experimental and theoretical studies on the transesterification of soybean oil with methanol catalyzed by zinc stearate. This reaction produces fatty acid methyl esters (FAME) and glycerol, and di- and monoglycerides as intermediate products.

Response Surface Methodology was used to study the relationship between process variables and triglyceride conversion, FAME yield and initial rate. An increase in the catalyst concentration and in the methanol/oil molar ratio increased triglyceride conversion and FAME yield and decreased the initial turnover frequency values. The latter was associated with the formation of an emulsion in the reaction medium.

A kinetic study of the reaction was performed. Two models were proposed. Model 1 assumed a complete mixing of the dissolved catalyst with the reactants and a second-order mechanism for the forward and reverse reactions, where the reaction system could be described as pseudo-homogeneous and the catalyst was dissolved in the reaction medium. Model 2 supposed that the dissolved catalyst formed part of a macro emulsion, with mass transfer resistance in the boundary layer around the droplets. The kinetic constants were determined, and Model 2 showed a better fit to the experimental data. The model and the kinetic parameters allow to generate reaction operation strategies.

1. Introduction

Biodiesel is defined as the monoalkyl esters derived from animal fats, plant based oils or algae oil, which is biodegradable. The substitution of traditional petroleum-based diesel fuel for this biofuel presents advantages, such as significantly lower emissions of carbon monoxide, aromatic hydrocarbons and particulate matter [1].

Industrially, the most common method for biodiesel production is the transesterification reaction, in which the oil or fat is reacted with a short chain alcohol in the presence of a homogeneous base catalysts (typically NaOH or KOH) [2]. The product is a mixture of fatty acid alkyl esters, and raw glycerol is obtained as co-product. The mixture of the formed esters is known as biodiesel, when it meets the established requirements (i.e. ASTM D6751, EN 14214, CAN/CGSB-3.524) [3]. Methanol and ethanol are commonly used alcohols [4]. The most important variables in biodiesel production were found to be [5]: reaction time, catalyst loading, reactants molar ratio and temperature. Low-cost feedstock contains high concentrations of free fatty acids (FFAs). When the concentration of FFAs is higher than 1 wt%, a esterification step using a homogeneous acid catalyst (usually H_2SO_4) is needed prior to the transesterification process [6]. Homogeneous acid catalysts require longer reaction time and could cause corrosion on equipment. Therefore, research on heterogeneous catalyst should be carried out extensively [7].

Over the past 10 years, the field of noncorrosive and recyclable catalysts related to biodiesel production has grown fast [8,9]. Inorganic acid solids are interesting catalysts for low quality feedstock, since they can simultaneously carry out the transesterification of triglycerides and esterification of FFAs. Compared to liquid acids, which have well-defined acid properties, solid acids can present a diversity of acid sites (Bronsted or Lewis acidity, with different strength and site density) [10]. Zeolites are among the different types of inorganic solids that have been used as catalysts for biodiesel production. Microporous zeolites are not completely

* Corresponding author. Departamento de Ingeniería Química, Universidad Nacional del Sur (UNS), Argentina.
E-mail address: gtonetto@plapiqui.edu.ar (G.M. Tonetto).

https://doi.org/10.1016/j.energy.2018.08.182
0360-5442/

Nomenclature

A	catalyst loading (%)
B	methanol/oil molar ratio (mol:mol)
C_i	concentration of component i (mol/l)
DG	diglycerides
d_i	diameter of the droplet i (μm)
FAME	fatty acid methyl esters
k_i	reaction rate constant for the reaction i ($l^2mol^{-1}min^{-1}g^{-1}$)
m	catalyst mass (g)
MG	monoglycerides
t	reaction time (min)
TG	triglycerides
V	reactor volume (l)
v_i	reaction rate of the reaction i (mol g^{-1} min^{-1})
X_{TG}	triglyceride conversion
Y_{FAME}	fatty acid methyl esters yield
κ	mass transfer coefficient (l g^{-1} min^{-1})

appropriate for this synthesis due to the diffusion limitation of glycerides inside the small pores [11,12]. The catalytic activity, stability and size- or shape selectivity of mesoporous zeolite and related materials are the focus of many recent studies. A zeolite-based catalyst was used to produce fatty acid methyl esters (FAME) from waste cooking oil, and it was able to simultaneously catalyze the esterification of fatty acids and the transesterification of triglycerides [13]. Under optimum reaction conditions, a conversion of 45% was achieved. On the other hand, using calcined Mg/Al hydrotalcite as catalyst in the transesterification of waste cooking oil, a 95% of FAME yield was obtained at 80 °C [14].

The performance of heteropolyacids (HPAs) has been investigated due to their high-water tolerance and acidity, even though HPAs can be slightly soluble in the reaction medium. The solid Cs2.5H0.5PW12O40 [15] showed a promising high activity comparable to that of conventional homogeneous catalysts. The immobilization of HPAs on a wide variety of supports to increase the surface area and hence improve the catalytic activity has also been studied [16]. Alcañiz-Monge et al. [17] studied the immobilization of the 12-tungstophosphoric heteropolyacid over zirconia supports in the esterification of palmitic acid with methanol, obtaining conversions above 90%. They observed leaching of the catalyst and the fouling of the surface.

Sulfated zirconia and tungstated zirconia have been extensively studied in the transesterification of vegetable oils [18,19]. As an alternative, sulfated zinc oxide as acid catalyst has also been examined [20], exhibiting a promising FAME yield of 80% at 65 °C and 4 h reaction time.

Among supported [21,22] or homogeneous [23,24] Lewis acid compounds, zinc plays an important role. $ZnCl_2$ supported on silica, alumina, niobia and charcoal was active in esterification reaction [25]. Zinc stearate immobilized on silica gel was a stable and active catalyst for simultaneous transesterification and esterification reactions [21]. At 200 °C and 10 h of reaction time, a FAME yield of 81% was obtained with a concentration of 1.6 wt.% FFA. In previous works, Reinoso et al. [26] showed the potential of zinc carboxylate as catalyst for the transesterification of soybean oil to produce biodiesel under mild experimental conditions. This compound with Lewis acid sites is soluble in the non-polar phase (oil and FAME) at reaction temperature and re-crystallizes at room temperature. Its flexible coordination geometry, fast ligand exchange, and its Lewis acid role are some of the features that make zinc an invaluable element in biological [27] and chemical [26] catalysis.

Aboelazayem et al. [28] studied the biodiesel production from castor oil with KOH as catalyst. The influence of the independent variables on the reaction response has been evaluated using Response Surface Methodology (RSM). Analysis of variance (ANOVA) has been used to investigate the adequacy of the predicted model. On the other hand, Response Surface Methodology (RSM) in aggregation with Central Composite Design (CCD) was employed to evaluate the best potential combination of catalyst concentration, methanol to oil molar ratio, reaction time and temperature for higher yield of biodiesel content using a non-edible dairy waste scum as feedstock [29]. Considering the catalytic potential of Zn carboxylic salts for biodiesel production, Response Surface Methodology was used in the present work to study the relationship between process variables (catalyst concentration and initial reactant ratio) and soybean oil conversion, FAME yield and initial rate.

It was observed that the studied catalyst (zinc stearate) forms a macroemulsion in the reaction medium that was studied in detail in order to understand the phenomenon. The catalyst is located at the interface of the emulsion droplet. Emulsion catalysis has been demonstrated to be a useful strategy for overcoming the compatibility of different media in the liquid-liquid biphasic reaction system [30]. Two mathematical models were also proposed for the methanolysis of soybean oil: one where the catalyst is dissolved and perfectly mixed in a pseudo-homogeneous reaction system, and a second one which takes into account that the catalyst is part of a self-organized system. The latter, is a simple and original mathematical model, that consider the mass transfer resistance present in this complex reaction system. The kinetic parameters were determined by fitting the models with the experimental results. The kinetic parameters and the reactor model permit to generate reaction operation strategies. The results would provide necessary data for the biodiesel production from soybean oil, which is one of most commonly used oils in the synthesis of this biofuel [31,32]. The originality of this work lies in the application of emulsion catalysis in biodiesel synthesis.

2. Material and methods

2.1. Catalyst preparation

The synthesis of zinc stearate ($Zn(C_{17}H_{35}COO)_2$, referred here as ZnEs) was carried out in an alcoholic solution [33]. The stearic acid (from Sigma Aldrich, 99%) and NaOH (Cicarelli, 97%) were mixed in stoichiometric amounts at 40 °C with constant magnetic stirring. Then $ZnCl_2$ (Biopack, 99%) was added dropwise. The obtained precipitate was filtered, washed with deionized water and dried for 24 h at 50 °C.

2.2. Catalytic tests

The transesterification tests were carried out in a 600 cm^3 Parr reactor (internal diameter: 64 mm) operated in batch mode, equipped with a 4-angled blade stirrer. The agitation rate was 500 rpm in order to perform the reaction in the absence of external mass transfer resistances [26]. Reactions were studied at 100 °C, with a reaction time of 120 min. Longer reaction times (360 and 480 min) were used for some tests in order to obtain data of the thermodynamic equilibrium. Temperature was selected considering that the catalyst is soluble in the non-polar phase (oil and FAME) at 100 °C, and re-crystallizes at lower temperatures. At higher values than 140 °C, the catalytic solid can be transformed into Zn glycerolate [34].

The pressure in the system for the transesterification reactions

corresponds to the vapor pressure of methanol: 52 psi at 100 °C.

Refined soybean oil (Argentinian commercial brand) without any special pretreatment and methanol (UVE HPLC) were used as reactants. Table 1 shows the fatty acid distribution of soybean oil obtained by gas chromatography. The values of the methanol/oil molar ratio were 10, 20 and 30, and of the catalyst loading were 1, 3 and 5 wt% (with respect to oil). In the catalytic tests, both parameters were established according to the experimental designs described below.

The soybean oil, the alcohol and the catalyst were fed into the reactor and then the system was heated until reaction temperature was reached. At that moment, the agitation was started and the zero-time sample was taken. The chromatography of the reactants and products was carried out according to the standard UNE-EN 14105 norm in a Perkin Elmer AutoSystem XL equipment with a ZB-5HT capillary column (15 m, 0.32 mm ID, 0.10 μm film thickness, with a pre-column of 2 m × 0.53 mm) and a FID detector.

The triglyceride conversion (X_{TG}) and FAME yield (Y_{FAME}) were calculated using the following equations:

$$X_{TG} = \frac{C_{TG}^{t0} - C_{TG}^{tf}}{C_{TG}^{t0}} 100 \quad (1)$$

$$Y_{FAME} = \frac{C_{FAME}^{tf}/3}{C_{TG}^{t0}} 100 \quad (2)$$

where C_{TG}^{t0} and C_{TG}^{tf} are the initial and final triglyceride concentrations (mol/l), respectively; and C_{FAME}^{tf} is the final FAME concentration (mol/l).

2.3. Experimental design

In order to evaluate the effects of the selected variables on the response variables, a mixed level 3^2 factorial design was developed with 2 centerpoint replicates, with a total of 8 experiments, as shown in Table 2. The order of the experiments was fully randomized to provide protection against the effects of lurking variables. The variables were methanol/oil molar ratio and catalyst loading. The levels studied for these variables are presented in Table 2. These levels were selected owing due to the advantage of working with low catalyst loadings and considering that transesterification is a reversible reaction, so the equilibrium can be shifted towards the products by using an excess alcohol.

Table 1
Fatty acid distribution of soybean oil.

Fatty acid	Composition (% wt.)
C16:0	11.0
C18:0	5.2
C18:1	25.7
C18:2	51.3
C18:3	4.9
C20:0	1.3
C22:0	0.5

Table 2
3^2 factorial design with two repetitions in the central point.

Test	Catalyst loading (A)	methanol/oil molar ratio (B)	Values	
			A (%)	B (mol:mol)
1	0	0	3	20
2	0	1	3	10
3	1	1	5	30
4	0	0	3	20
5	0	−1	3	10
6	1	−1	5	10
7	−1	−1	1	10
8	−1	1	1	30

The studied responses were triglyceride conversion and FAME yield at 1 h reaction time, and initial TOF. The software STATGRAPHICS Centurion version XV.2 was used for both the experimental design and the statistical analysis. The responses were adjusted by multiple regression, and the generated models were used to evaluate the effect of the selected experimental factors. The goodness of fit was assessed using the coefficient of determination (R^2). The statistically significant effect of the variables was tested using ANOVA. Non-significant coefficients were removed (p-value > 0.05), and the models were refined in order to consider only the statistically significant effects.

2.4. Characterization of the droplets formed in emulsion

Four representative oil-methanol mixtures were prepared. In all cases the oil-methanol molar ratio was 30 and the catalyst loading was 0, 1, 3 and 5%wt. The polar phase was dyed with an appropriate dye.

The droplets were observed using a Carl Zeiss polarized light microscope (ZeissPhomi III POL). The samples were placed onto microscope slides, covered with glass cover slips, and observed at ×160 magnification in transmission mode. At least 3 replicates were prepared for each sample. The volume-surface mean diameter (d_{32}) of the droplets was calculated using Equation (3), considering that the oil droplets were spherical:

$$d_{32} = \frac{\sum n_i d_i^3}{\sum n_i d_i^2} \quad (3)$$

where n_i was the number of droplets with diameter d_i.

3. Kinetic modelling

The transesterification of triglycerides (TG) is a sequence of three consecutive reversible reactions, in which diglycerides (DG) and monoglycerides (MG) are formed as intermediate compounds, and fatty acid methyl esters and glycerol (Gl) are formed as products. The reactions involved are:

$$TG + MOH \underset{k_{-1}}{\overset{k_1}{\longleftrightarrow}} DG + FAME \quad (4)$$

$$DG + MOH \underset{k_{-2}}{\overset{k_2}{\longleftrightarrow}} MG + FAME \quad (5)$$

$$MG + MOH \underset{k_{-3}}{\overset{k_3}{\longleftrightarrow}} Gl + FAME \quad (6)$$

The kinetics of the transesterification reaction can be described considering second-order kinetics (first-order for each compound involved in the reaction) [35,36]. The rate expressions are as follow:

$$v1 = k_1 C_{TG} C_{MOH} - k_{-1} C_{DG} C_{FAME} \quad (7)$$

$$v2 = k_2 C_{DG} C_{MOH} - k_{-2} C_{MG} C_{FAME} \quad (8)$$

$$v3 = k_3 C_{MG} C_{MOH} - k_{-3} C_{Gl} C_{FAME} \quad (9)$$

where MOH is methanol, C_i refers to the concentration of the corresponding species (mol l^{-1}), v_i is the reaction rate (mol g^{-1} min^{-1}), and k_i and k_{-i} are the reaction rate constants for forward and reverse reactions ($l^2 mol^{-1} min^{-1} g^{-1}$).

3.1. Model 1

The reactor used in the tests can be modeled as an ideal batch reactor. The hypotheses considered for the reactor model were as follows:

1. Perfect mixture of reactants and products in the tank, ensuring a uniform composition.
2. The reaction mixture can be considered as a pseudo-homogeneous system.
3. Isothermal reactor.
4. The catalyst is dissolved in the reaction medium and perfectly mixed. There is no mass transfer limitation. The overall process is kinetically controlled.
5. The methanol concentration is constant during the reaction and equal to the initial concentration.

Experiences not shown in the present work revealed the high mixing performance of the reactor [26]. For a well-agitated batch reactor, the mass balances of the species can be written as follows:

$$\frac{dC_{TG}}{dt} = -v1 \frac{m}{V} \quad (10)$$

$$\frac{dC_{MOH}}{dt} = 0 \quad (11)$$

$$\frac{dC_{DG}}{dt} = (v1 - v2) \frac{m}{V} \quad (12)$$

$$\frac{dC_{FAME}}{dt} = (v1 + v2 + v3) \frac{m}{V} \quad (13)$$

$$\frac{dC_{MG}}{dt} = (v2 - v3) \frac{m}{V} \quad (14)$$

$$\frac{dC_{Gl}}{dt} = v3 \frac{m}{V} \quad (15)$$

where m is the catalyst mass (g), V is the reactor volume (l), and t is the reaction time (min).

3.2. Model 2

In order to improve the model and explain the overall process better, a second reactor model was studied. Hypotheses 1–3 were maintained, and the rest of the hypotheses were changed as follows (taking into account the results from section 4.1):

4. The catalyst is part of a self-organized system. There is mass transfer resistance in the boundary layer around the droplets.
5. The internal phase of the droplets consists only of methanol.
6. The reaction occurs only in the interphase of the droplets of the organized system (see scheme in Fig. 6).

The equations that represent the reactor are:

$$\frac{dC_{TG}}{dt} = \kappa (C_{TG} - C^s_{TG}) \frac{m}{V} = -v1 \frac{m}{V} \quad (16)$$

$$\frac{dC_{MOH}}{dt} = 0 \quad (17)$$

$$\frac{dC_{DG}}{dt} = \kappa (C_{DG} - C^s_{DG}) \frac{m}{V} = (v1 - v2) \frac{m}{V} \quad (18)$$

$$\frac{dC_{FAME}}{dt} = \kappa (C_{FAME} - C^s_{FAME}) \frac{m}{V} = (v1 + v2 + v3) \frac{m}{V} \quad (19)$$

$$\frac{dC_{MG}}{dt} = \kappa (C_{MG} - C^s_{MG}) \frac{m}{V} = (v2 - v3) \frac{m}{V} \quad (20)$$

$$\frac{dC_{Gl}}{dt} = \kappa (C_{Gl} - C^s_{Gl}) \frac{m}{V} = v3 \frac{m}{V} \quad (21)$$

where C^s_i and C_i refer to the concentration of the corresponding species on the droplet surface and in the bulk reaction medium. In the case of methanol, C^s_{MOH} represents pure methanol. κ represents the mass transfer coefficient for the glycerides and FAME in the proximity of the surface of the droplets, and is expressed by the following equation:

$$\kappa = \alpha + \beta \cdot m \quad (22)$$

where α and β are constants and m is the catalyst loading (g). Eq. (22) is derived from the result of the experimental design reported in section 4.2.

For both models, the catalyst is assumed to be dissolved in the reaction medium. In the case of Model 1, a perfect mixing of the catalyst with the reagents is also assumed (pseudo-homogeneous system). For the second reactor model, the catalyst is assumed to be part of an organized system, which makes the contact between the reagents difficult. These hypotheses in Model 2 take into account a real phenomenon that takes place as a consequence of the chemical nature of the catalyst.

3.3. Numerical and statistical resolution

The Gproms software was used to solve the set of algebraic and differential equations, and to fit the experimental data. It is based on the statistical method of maximum likelihood estimation [37]. The coefficient of determination (r^2) gives the fitting quality, and it was calculated using the following equation:

$$r^2 = \frac{\sum_{i=1}^{n} \left(C_i^{calc} - \overline{C} \right)^2}{\sum_{i=1}^{n} \left(C_i - \overline{C} \right)^2} \quad (23)$$

The model adequacy and the discrimination between models were determined using the model selection criterion (MSC), according to the following equation:

$$MSC = ln \left[\frac{\sum_{i=1}^{n} \left(C_i - \overline{C} \right)^2}{\sum_{i=1}^{n} \left(C_i - C_i^{calc} \right)^2} \right] - \frac{2p}{n} \quad (24)$$

where n is the number of experimental data, p is the total of fitted parameters, $\overline{C}$ is the average relative concentration and C_i^{calc} and C_i are the predicted and the experimental values, respectively. When various different models are compared, the most significant one is

that which leads to the highest MSC and r^2 values.

4. Results and discussion

4.1. Triglyceride conversion and FAME yield

Table 3 shows triglyceride conversion (X_{TG}) and FAME yield (Y_{FAME}) after 60 min reaction time for the proposed experimental design. X_{TG} and Y_{FAME} present values between 42 and 82% and 20 and 57%, respectively. The zinc carboxylic salt was able to catalyze the triglyceride transesterification with good activity and selectivity under mild operating conditions.

The quadratic model obtained from the fitted experimental data for X_{TG} is presented in Eq. (25). This model was adjusted by stepwise selection (Fisher's test), removing variables in order to find the best model containing only statistically significant variables. Since the P-value for each variable was less than 0.05, there was a statistically significant relationship between the variables and the response with a confidence level greater than 95.0%. The R^2 statistic indicates that the model as fitted accounts for 97.3% of the variability in triglyceride conversion. Table 4 shows the standard errors, t values and p values of all the coefficients.

$$XTG = 20.19 + 24.19A + 0.04B^2 - 0.30AB - 2.08A^2 \quad (25)$$

The minus sign for the terms A*B and A^2 allow Eq. (25) (a second order polynomial equation) to represent the low effect that A and B have on X_{TG} when A and B have their highest values. A response surface plot for the second order model at 60 min reaction time is shown in Fig. 1 a, presenting the effects of the amount of catalyst and methanol/oil molar ratio. Fig. 1 a shows that the molar ratio of the reactants (B) affects the TG conversion when the catalyst concentration (A) is low. At high catalyst loadings (A), the effect of B is less noticeable. In turn, the simultaneous increasing of both variables leads to higher TG conversion values.

In the case of FAME yield, only two effects have P-values less than 0.05, indicating that there is a statistically significant relationship between the variables at the 95.0% confidence level. Eq. (26) shows the linear model obtained to adjust the data and Table 5 shows the standard errors, t values and p values of the coefficients.

$$Y_{FAME} = 8.44 + 5.89A + 0.65B \quad (26)$$

The R^2 statistic indicates that the model as fitted accounts for 96.04% of the variability in Y_{FAME}, thus a good fit of the selectivity values was obtained with this simple model. Fig. 1 b presents a response surface plot obtained from Eq. (26). It shows that both variables have a significant effect on Y_{FAME} in the studied range. The highest yield was obtained for the highest values of each variable.

The maximum values of TG conversion and FAME yield were achieved with the studied maximum value for each factor (A = 5%, B = 30 mol:mol). It can be observed that an increase in the methanol/oil molar ratio generates a positive effect on both studied responses. This behavior is typical of reversible reactions, where an excess of reactants will favor the product formation.

On the other hand, Fig. 2 shows the parity plot of the calculated vs. experimental TG conversion (a) and FAME yield (b) for all the experimental tests. It can be observed a suitable fit of the experimental data.

4.2. Initial rates

Initial rates were evaluated as turn over frequencies (TOF, calculated as reacted TG moles per mole of catalyst per time). Table 6 shows initial TOF values at different catalyst loadings (A) and methanol/oil molar ratios (B).

Equation (27) describes the relationship between the TOF and the studied variables; it was obtained by fitting the data with a second-order model and refined to include only significant variables. Table 7 shows the standard errors, t values and p values of all the coefficients.

$$TOF\left(s^{-1}\right) = 0.065 - 0.034A + 0.004B + 0.005A^2 - 0.001AB \quad (27)$$

Since the ANOVA P-value is less than 0.05, there is a statistically significant relationship between the variables at the 95.0% confidence level. The R^2 statistic indicates that the model explains accounts for 98.8% of the variability in TOF. Fig. 3 shows a response surface plot obtained from Eq. (27), where reaction time was set at 20 min and the other factors were varied.

Fig. 4 shows the calculated vs. experimental TOF. It can be observed that the model describes satisfactorily the TOF behavior.

In a previous work [26], it was shown that Zn stearate is completely dissolved in oil and FAME and it is insoluble in methanol and glycerol at reaction temperature. Thus, the reaction was carried out in two immiscible liquid phases, with the catalyst dissolved in the non-polar phase. On the other hand, as previously mentioned, the triglyceride conversion and FAME yield were independent of the agitation rate above 500 rpm, ensuring that there was no external mass transfer resistance [26]. When Fig. 3 is analyzed, it can be observed that an increase in the reactant molar ratio produces an improvement in TOF, and this effect is more marked at low catalyst loadings. However, the TOF values noticeably decrease as the amount of catalyst is increased (at constant methanol/oil molar ratio).

This behavior could be explained by the formation of a self-organized system (i.e. a macroemulsion), which under some circumstances, hinders contact between the reactants. Zinc stearate has both hydrophilic (the carboxylate) and hydrophobic (the long hydrocarbon chain) groups. Therefore, the catalyst can interact with both phases in the reactant medium in order to partially avoid phase separation and stabilize the thermodynamically unstable systems.

Table 3
Experimental results of catalytic test: triglyceride conversion and FAME yield (reaction time: 60 min, temperature: 100 °C).

Test	Experimental variables		Experimental results (%)	
	Catalyst loading (%)	methanol/oil molar ratio (mol:mol)	X_{TG}	Y_{FAME}
1	3	20	72	37
2	3	30	80	47
3	5	30	82	57
4	3	20	73	37
5	3	10	72	37
6	5	10	77	44
7	1	10	42	20
8	1	30	71	34

Table 4
Standard errors, t values and p values of all the coefficients obtained with the quadratic model for TG conversion.

Parameter	Standard Error	T Statistic	P-Value
CONSTANT	5.98545	3.37265	0.0433
A	3.97663	6.08393	0.0089
B^2	0.00658796	6.0545	0.0090
A B	0.0775511	−3.80846	0.0318
A^2	0.563873	−3.69181	0.0345

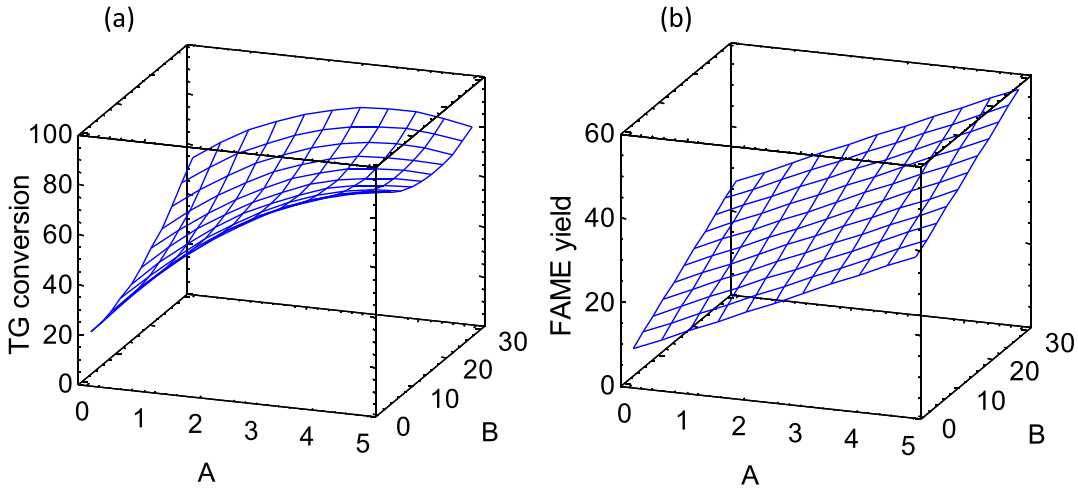

Fig. 1. Response surface for the triglyceride conversion (a) and FAME yield (b) in the transesterification of soybean oil (reaction time: 60 min). Variables: A: catalyst loading (%) and B: methanol/oil molar ratio (mol:mol).

Table 5
Standard errors, t values and p values of all the coefficients obtained with the quadratic model for TG conversion.

Parameter	Standard Error	T Statistic	P-Value
CONSTANT	2.99588	2.81692	0.0372
A	0.643619	9.14944	0.0003
B	0.105102	6.15272	0.0016

It is known that the emulsion reaction medium is favorable for the improvement of the mass diffusion limitations in liquid multiphase systems caused by reactants being located in the different phases [38,39]. It has been reported that the formation of more emulsion droplets with smaller size can efficiently disperse the substrate in the emulsion droplets, increasing the initial rate [40]. In this case, the increase of the catalyst loading originated fewer droplets with a bigger size (next section).

According to Fig. 3, when high catalyst concentrations are used in the reaction test, apparently the catalyst is not properly used in terms of initial rate. This issue will be studied in the next section.

4.2.1. Droplet size measurement

Fig. 5 shows images of the microstructures of the four oil-methanol mixtures (described in Section 2.4) captured under an optical microscope. They reveal the presence of spherical droplets surrounded by a continuous phase. As it can be observed, the center of the droplets is dark (corresponding to previously-colored methanol), indicating that the dispersed phase is alcohol and the

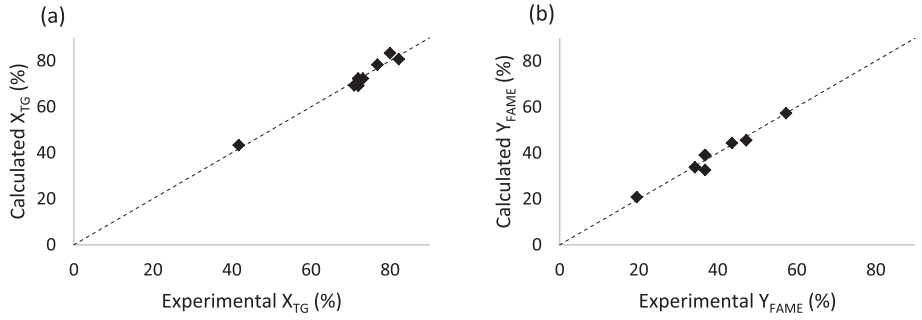

Fig. 2. Parity plot of the calculated vs. experimental TG conversion (a) and FAME yield (b).

Table 6
Experimental results of catalytic test: turnover frequency.

Test	Experimental variables		Experimental results
	Catalyst loading (%)	methanol/oil molar ratio (mol:mol)	TOF (s^{-1})
1	3	20	0.029
2	3	30	0.048
3	5	30	0.019
4	3	20	0.036
5	3	10	0.027
6	5	10	0.013
7	1	10	0.062
8	1	30	0.123

Table 7
Standard errors, t values and p values of all the coefficients obtained with the quadratic model for TOF.

Parameter	Standard Error	T Statistic	P-Value
CONSTANT	0.0131868	4.93708	0.0159
A	0.00697677	−4.90915	0.0162
B	0.000496894	7.10245	0.0057
A^2	0.00102867	4.67838	0.0184
A B	0.000145476	−4.72587	0.0180

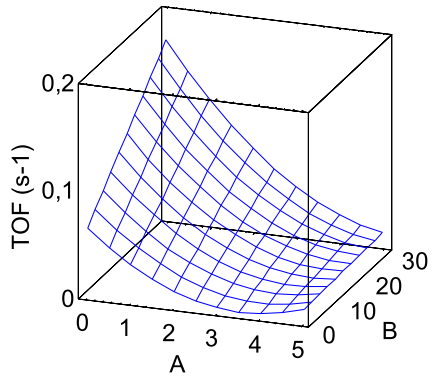

Fig. 3. Response surface for the TOF using a quadratic model. Variables: A: catalyst loading (%) B: and methanol/oil molar ratio (mol:mol).

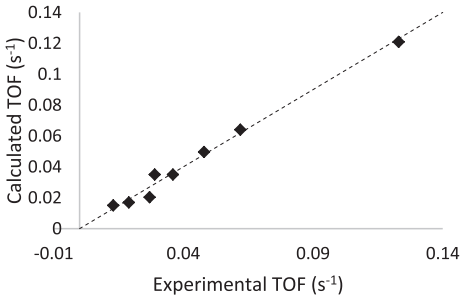

Fig. 4. Parity plot of the calculated vs. experimental TOF.

continuous phase is the oil. A water-in-oil (W/O) emulsion is sometimes called an inverse emulsion, where the hydrophobic tails of the catalyst are in contact with the oil and the hydrophilic heads are in contact with the dispersed phase (scheme in Fig. 6). Whether an emulsion of oil and water turns into a W/O emulsion or an "oil-in-water" emulsion depends on the volume fraction of both phases (equal in this case) and the type of surfactant present in the emulsion. For this system, the Bancroft rule applies and the phase in which the Zn stearate is more soluble constitutes the continuous phase.

The pictures in Fig. 5 show that the samples were polydisperse emulsions with different oil droplet sizes. Table 8 shows the d_{32} diameters of the droplets and the arithmetic mean diameter, which were measured using image analysis of the microstructures. The arithmetic mean diameters of the droplets varied between 22.3 ± 1.6 and 64.1 ± 14.1 μm, while the d_{32} presented values between 39.5 and 108.7 μm. These values are much higher than the arithmetic mean diameters since the volumetric diameter confers more weight to the larger drops. The largest and smallest droplet sizes were observed for samples with 5% and 1% of catalyst, respectively. Due to the observed droplet sizes, the emulsion can be considered a macroemulsion, and it remains stable due to the presence of the zinc carboxylate (anionic surfactant) [41]. When 0.5% of catalyst was analyzed, no emulsion was formed. Thus, for this system, the critical micelle concentration of zinc stearate is in the range of 3.2–6.5 mM, according to reported values for anionic surfactants [42].

In the sample without catalyst, once the agitation was stopped, all the droplets coalesced, and two continuous phases were formed instead of a dispersed phase in a continuous phase, as shown in Fig. 5 d.

This observation allows us to infer the behavior of the catalyst and reactants/products in the reaction medium. It appears that the higher the catalyst loading, the larger the size of the observed droplets. This behavior was previously reported by Lucena et al. [43] for the micellar system formed by a nonylphenolpolyethoxylated surfactant (Ultranex-50) in organic solvents (octane, decane and dodecane), using ethylene glycol monobutyl ether as polar additive. They observed that the reverse micelle size (hydrodynamic radius) significantly increased with surfactant concentration for all the solvents used.

Water-in-oil (W/O) emulsions are not so studied as oil-in-water emulsions. In general, W/O emulsions present low stability because of the high mobility of water droplets, which can easily sediment, flocculate or coalesce [44]. In the case presented in this work, the macroemulsion is remarkably stable. A better understanding of the interactions between the components of this emulsion would help to understand the mass transfer phenomena that affect the reaction system, which would have great applicability due to its good performance with low-cost oils [32].

4.3. Kinetic modelling

The models were applied for correlating the experimental data obtained at different catalyst loadings and reactant molar ratios. Model 1 assumes a complete mixing of the dissolved catalyst with the reactants and a second-order mechanism for the forward and reverse reactions, where the reaction system could be described as a pseudo-homogeneous catalyzed reaction. Model 2 assumes that the catalyst is dissolved in the reaction medium, and that it is part of a self-organized system, with mass transfer resistance in the boundary layer around the droplets.

The kinetic parameters fitted for both kinetic models are shown in Table 9. The estimates of the kinetic constants were significantly different from zero. The coefficient of determination (r^2) gives the fitting quality (i.e., the percentage of explanation of the total data variation around the observed average value). R^2 presented values of 0.92 and 0.96 for Model 1 and 2, respectively. Additionally, when various different models are compared, the most significant one is that which leads to the highest value of the model selection criterion (MSC). This parameter was 2.6 and 3.1 for Model 1 and 2, respectively.

The best agreement between the experimental data and predicted values (high r^2 and MSC values, positive estimates, and positive left limits at 95% confidence or more) was obtained with Model 2. In summary, the best model to interpret the transesterification of vegetable oil catalyzed by Zn stearate is that which considers the formation of a self-organized system, due to the chemical nature of the catalyst, and the mass transfer resistance in the boundary layer around the droplets.

Table 9 shows the following relationship between the kinetic constants involved in the transesterification reaction at the studied temperature (for Model 2):

$k_3 > k_1 > k_2$ and $k_{-3} > k_{-1} > k_{-2}$

The equilibrium constants determined at 100 °C have the following order:

$K_{eq,2} > K_{eq,1} > K_{eq,3}$

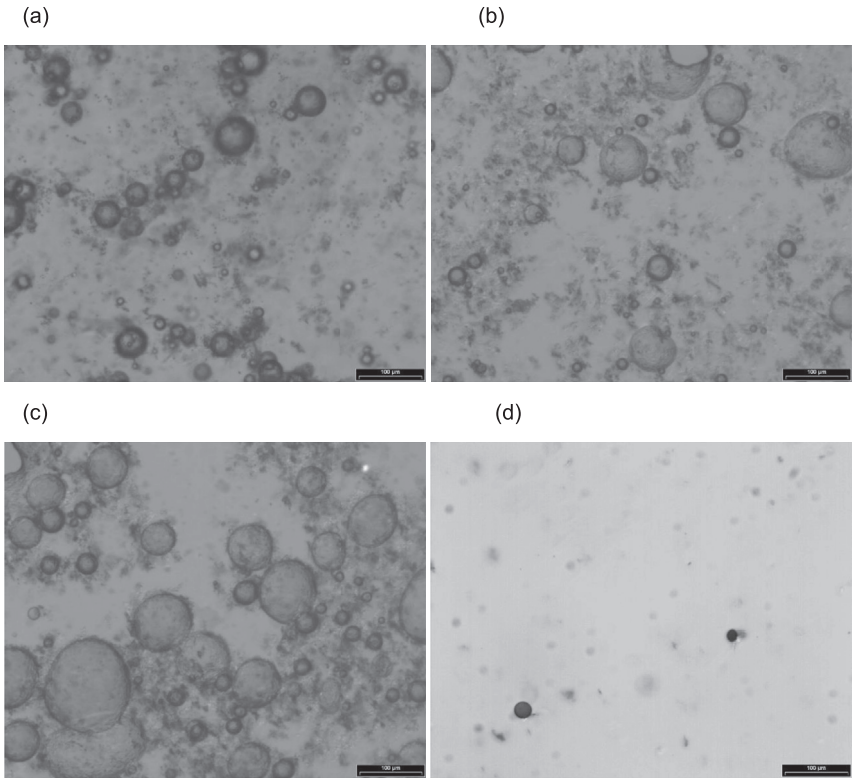

Fig. 5. Optical microscopy images (x160) of different samples composed by methanol, soybean oil (molar relation: 30) and 1% (a), 3% (b), 5% (c), and 0% (d) of zinc stearate. Scale bar = 100 μm.

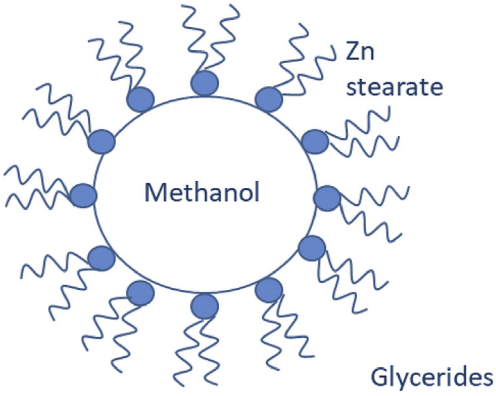

Fig. 6. Schematic model of the organized system presented in the reaction volume.

Table 8
Mean droplet diameter, d_{32} and arithmetic, of W/O emulsions stabilized by the Zn stearate.

Sample	Diameter (μm)	
	d_{32}	Main arithmetic
1%	39.5 ± 4.6	22,3 ± 1,6
3%	58.8 ± 8.8	33,9 ± 3,94
5%	108.7 ± 25.7	64,1 ± 14,1

Due to the nature of the studied catalyst, it is not easy to compare these results with the values found in the literature. For the same reaction catalyzed by zinc aluminate [45], the following kinetic constants were reported: $k_1 = 3.4\ 10^{-8}$, $k_2 = 1.4\ 10^{-8}$, $k_3 = 1.1\ 10^{-7}$, $k_{-1} = 9.0\ 10^{-9}$, $k_{-2} = 1.7\ 10^{-8}$ and $k_{-3} = 9.2\ 10^{-8}$ $l^2mol^{-1}min^{-1}g^{-1}$ (at 100 °C). These values are significantly lower than those found in this work, highlighting the good activity of the Zn carboxylate that is dissolved in the reaction medium, but that can be easily separated after use.

Table 9
Kinetic parameters fitted for Models 1 and 2, with the corresponding confidence intervals of 95%, for soybean oil transesterifcation catalyzed by Zn stearate. Temperature: 100 °C.

Parameter	Model 1	Model 2
MSC	2.6	3.1
r^2	0.92	0.96
k_1 ($l^2mol^{-1}min^{-1}g^{-1}$)	$2.74\ 10^{-1} \pm 7.47\ 10^{-5}$	$1.74\ 10^{-4} \pm 1.73\ 10^{-6}$
k_2 ($l^2mol^{-1}min^{-1}g^{-1}$)	$2.26\ 10^{-1} \pm 6.97\ 10^{-5}$	$1.57\ 10^{-4} \pm 1.26\ 10^{-6}$
k_3 ($l^2mol^{-1}min^{-1}g^{-1}$)	$4.96\ 10^{-1} \pm 4.56\ 10^{-4}$	$2.68\ 10^{-4} \pm 1.69\ 10^{-6}$
k_{-1} ($l^2mol^{-1}min^{-1}g^{-1}$)	$1.49 \pm 1.89\ 10^{-3}$	$3.43\ 10^{-4} \pm 1.66\ 10^{-5}$
k_{-2} ($l^2mol^{-1}min^{-1}g^{-1}$)	$4.17\ 10^{-1} \pm 1.01\ 10^{-3}$	$2.87\ 10^{-4} \pm 9.24\ 10^{-6}$
k_{-3} ($l^2mol^{-1}min^{-1}g^{-1}$)	$2.32 \pm 2.93\ 10^{-3}$	$1.30\ 10^{-3} \pm 1.13\ 10^{-5}$
$K_{eq,1}$	0.184	0.508
$K_{eq,2}$	0.543	0.549
$K_{eq,3}$	0.214	0.206
α	–	$1.18\ 10^{-2}$
β	–	$-2.61\ 10^{-3}$

In the case of reference [41], the equilibrium constants $K_{eq,1}$, $K_{eq,2}$ and $K_{eq,3}$ were 0.1, 0.76 and 0.33, respectively. On the other hand, Karmee et al. [46] reported $K_{eq,1} = 0.15$, $K_{eq,2} = 0.79$ and $K_{eq,3} = 0.11$, also at 100 °C. The results presented in this work are in good agreement with those values.

The results obtained with the proposed model under different experimental conditions for the transesterification of soybean oil with methanol are presented in Figs. 7 and 8, where the dashed lines correspond to the calculated values, and the symbols

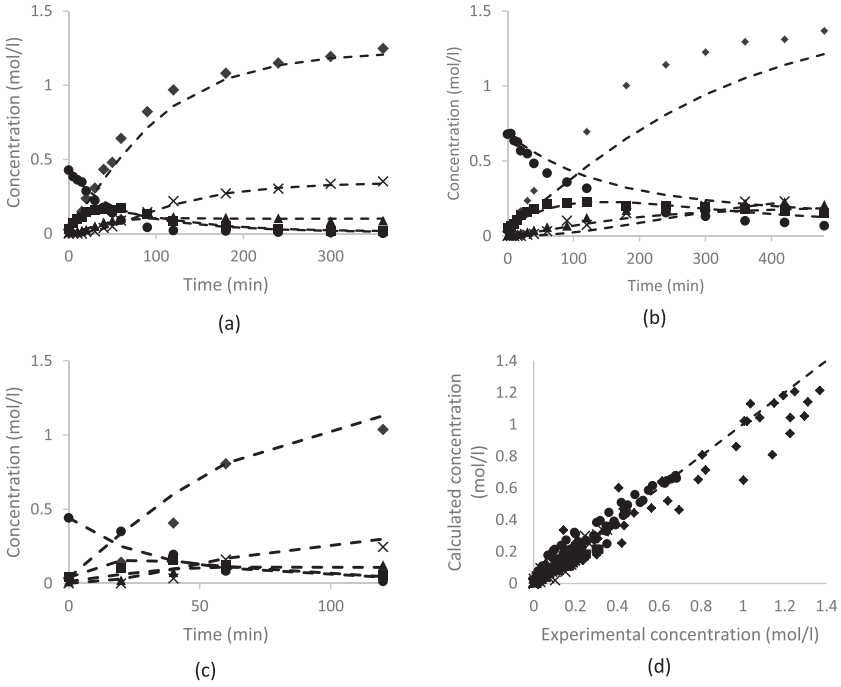

Fig. 7. MODEL 1 - Product and reactant distribution in the transesterification of soybean oil catalyzed by zinc stearate at 100 °C. Operating conditions: (a) Catalyst loading = 3%, methanol/oil molar ratio 30; (b) Catalyst loading = 1%, methanol/oil molar ratio 10; (c) Catalyst loading = 5%, methanol/oil molar ratio 30; (d) Parity plot of the calculated vs. experimental concentrations. Ref.: Curves: simulation, Symbols: experimental data, ●TG; ■ DG; ◆ FAME; ▲ MG; x GLY.

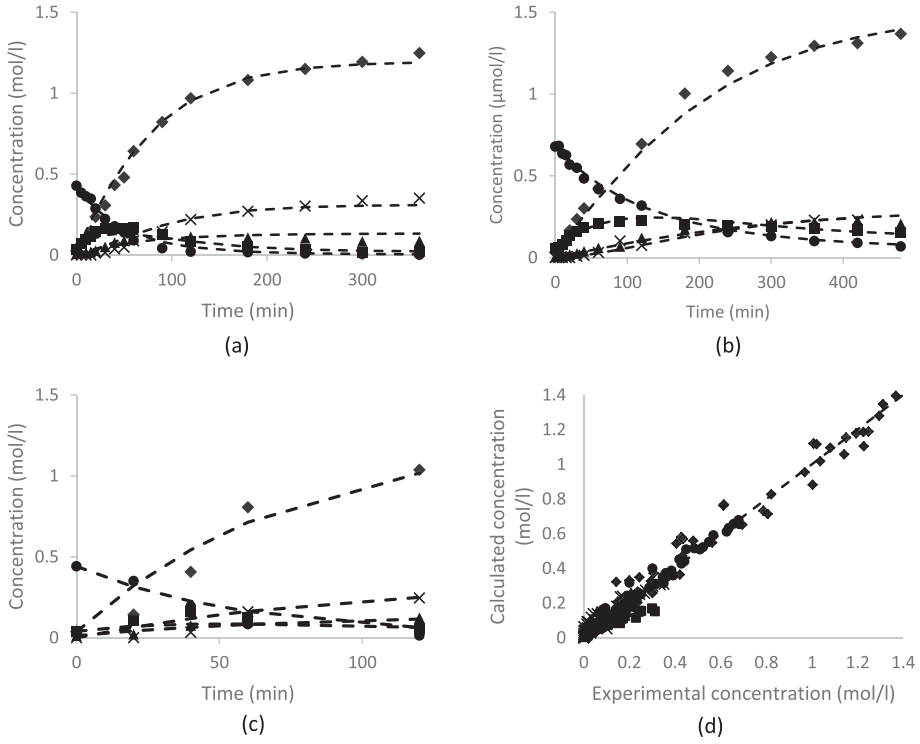

Fig. 8. MODEL 2 - Product and reactant distribution in the transesterification of soybean oil catalyzed by zinc stearate at 100 °C. Operating conditions: (a) Catalyst loading = 3%, methanol/oil molar ratio 30; (b) Catalyst loading = 1%, methanol/oil molar ratio 10; (c) Catalyst loading = 5%, methanol/oil molar ratio 30; (d) Parity plot of the calculated vs. experimental concentrations. Ref.: Curves: simulation, Symbols: experimental data, ●TG; ■ DG; ◆ FAME; ▲ MG; x GLY.

represent the experimental data. There is a reasonable fit between the models and the experimental data, especially in the case of Model 2. It can be observed that Model 2 satisfactorily describes the transesterification kinetics for this catalyst. This is confirmed in Fig. 8 d for all the experimental tests.

In the case of FAME concentrations at A = 1% and B = 10 (Fig. 7b), it can be observed that Model 1 predicts a lower concentration than the experimental data. These results correspond to

the operating conditions with the lowest catalyst loading and methanol concentration. At a low catalyst concentration, with a smaller droplet size, the mathematical model appears to underestimate the FAME generation and the oil conversion. The same behavior was observed with the test at A = 1% and B = 30 (not shown in this manuscript).

Regarding the mass transfer coefficient, κ, for the glycerides and FAME in the proximity of the surface of the drop, the values of α and β constants (in Eq. (22)) were statistically significant:

$$\kappa = 1.18\ 10^{-2} - 2.61\ 10^{-3}.m \quad (28)$$

κ value is expressed as l/min. g and its value was 0.01, 0.005 and 0.001 for 1, 3 and 5% catalyst, respectively. It is observed that κ increases as the catalyst loading decreases, which is in perfect agreement with the previous observation, where TOF decreases with the catalyst loading.

This would indicate that an increase in the catalyst loading leads to more important diffusional problems, with an increase in the mass transfer resistance due to the formation of bigger droplets in the macroemulsion, thus making the contact between the reactants more difficult. However, if the overall reaction system is considered, an increase in the catalyst loading generates an increase in triglyceride conversion. That is to say, globally the effect of the increase in the amount of catalyst on the conversion is greater than on the mass transfer resistance. In previous studies, the effect of methanol concentration was considered in Eq. (28), but the mathematical calculus indicated that its effect was negligible.

The mathematical model is a very useful tool to generate operating strategies for the reaction process. From the data reported in this study, it was possible to determine by simulation that, a maximum FAME yield of 90% can be obtained at 100 °C and 360 min (A = 3%, B = 30) in one stage. In biodiesel industrial plants, it is desirable to reach high conversion in short reaction times. To achieve this aim, two-step batch-wise operating units are frequently used, with each step consisting of a batch reactor and a settling tank (for glycerol separation). In the present case, a FAME yield of 90% can be obtained using a two-stage process for a shorter reaction time (120 min in each stage), saving 120 min of reaction time of the transesterification reaction at 100 °C, and the corresponding energy cost. Compared with the conventional base homogeneous process, the advantage of our proposed model is that it is not necessary to add more catalyst, and better-quality glycerol can be obtained. The concentration of FAME required according to ASTM D6751 is 96.5%. By three reaction stages of 120 min each, it was possible to achieve a TG conversion of 99% and a FAME yield of 96%, according to the results of Model 2, for a reaction with 3% catalyst loading and alcohol to oil molar ratio of 30.

5. Conclusion

Due to environmental restrictions, fuel production using renewable resources such as vegetable oils is considered. Soybean oil is one of most used oils in the synthesis of biodiesel.

The purpose of this study was to gain a better understanding of the performance of zinc stearate as an environmentally-friendly catalyst in the transesterification of soybean oil with methanol. Experimental and theoretical studies were carried out using Response Surface Methodology and kinetic modelling. Based on the data presented, the following conclusions may be drawn:

1. An increase in the catalyst concentration and reactant molar ratio enhanced the triglyceride conversion and FAME yield. The obtained results also showed that an increase in catalyst concentration decreased the initial TOF.
2. The latter was related to the formation of an inverse emulsion due to the surfactant properties of the catalyst. It was observed that the increase in catalyst loading produced fewer droplets with larger size.
3. The kinetics of soybean oil transesterification catalyzed by zinc stearate was modeled considering a second-order mechanism for the forward and reverse reactions, where the reaction system can be described as a pseudo-homogeneous catalyzed reaction. The best model for interpreting the experimental results was the one that considered the formation of a self-organized system, due to the chemical nature of the catalyst, with mass transfer resistance in the boundary layer around the droplets.
4. The simulated results were in agreement with the experimental data.
5. The kinetic parameters and the proposed reactor model can be used to generate operational strategies, such as operating with two reactors in series. In this way, the strategies can be proposed to achieve biodiesel within international quality standards such as ASTM. The catalyst can be recovered after reaction, and biodiesel of better quality could be obtained.

This work demonstrates that emulsion catalysis is a very useful strategy for the production of biodiesel.

Considering the need for low-cost fuel with low environmental impact, future works will focus on the application of zinc stearate as catalyst to obtain second-generation biodiesel at different temperatures and reaction time in order to achieve biodiesel of standard quality.

Acknowledgements

The authors thank the Agencia Nacional de Promoción Científica y Tecnológica (National Agency of Scientific and Technological Promotion, Argentina) and the Consejo Nacional de Investigaciones Científicas y Técnicas (National Council for Scientific and Technological Research, CONICET) for the financial support.

References

[1] Bart JCJ, Palmeri N, Cavallaro S. Biodiesel science and technology: from soil to oil. first ed. Woodhead Publishing; 2010.
[2] Narula V, Khan MF, Negi A, Kalra S, Thakur A, Jain S. Low temperature optimization of biodiesel production from algal oil using CaO and CaO/Al2O3 as catalyst by the application of response surface methodology. Energy 2017;140:879–84.
[3] Barabás I, Todorut I. Biodiesel quality, standards and properties. Biodiesel-quality, emissions and by-products. InTech; 2011.
[4] Sanli H, Canakci M. Effects of different alcohol and catalyst usage on biodiesel production from different vegetable oils. Energy Fuels 2008;22:2713–9.
[5] Alper Tapan N, Yıldırım R, Erdem Günay M. Analysis of past experimental data in literature to determine conditions for high performance in biodiesel production. Biofuels Bioprod Biorefin 2016;10:422–34.
[6] Pua FL, Fang Z, Zakaria S, Guo F, Chia CH. Direct production of biodiesel from high-acid value Jatropha oil with solid acid catalyst derived from lignin. Biotechnol Biofuels 2011;4:56.
[7] Lam MK, Lee KT, Mohamed AR. Homogeneous, heterogeneous and enzymatic catalysis for transesterification of high free fatty acid oil (waste cooking oil) to biodiesel: a review. Biotechnol Adv 2010;28:500–18.
[8] Baskar G, Aiswarya R. Trends in catalytic production of biodiesel from various feedstocks. Renew Sustain Energy Rev 2016;57:496–504.
[9] Avhad MR, Marchetti JM. Innovation in solid heterogeneous catalysis for the generation of economically viable and ecofriendly biodiesel: a review. Catal Rev 2016;58:157–208.
[10] Wilson K, Adams DJ, Rothenberg G, Clark JH. Comparative study of phenol alkylation mechanisms using homogeneous and silica-supported boron trifluoride catalysts. J Mol Catal Chem 2000;159:309–14.
[11] Sani YM, Daud WMAW, Aziz ARA. Activity of solid acid catalysts for biodiesel production: a critical review. Appl Catal A 2014;470:140–61.
[12] Carrero A, Vicente G, Rodríguez R, Linares M, del Peso GL. Hierarchical zeolites as catalysts for biodiesel production from Nannochloropsis microalga oil. Catal Today 2011;167:148–53.
[13] Hassani M, Najafpour N, Mohammadi M, Rabiee SM. Preparation, characterization and application of zeolite-based catalyst for production of biodiesel

from waste cooking oil. J Sci Ind Res 2014;73:129–33.
[14] Ma Y, Wang Q, Zheng L, Gao Z, Wang Q, Ma Y. Mixed methanol/ethanol on transesterification of waste cooking oil using Mg/Al hydrotalcite catalyst. Energy 2016;107:523–31.
[15] Chai F, Cao F, Zhai F, Chen Y, Wang W, Su Z. Transesterification of vegetable oil to biodiesel using a heteropolyacid solid catalyst. Adv Synth Catal 2007;349:1057–65.
[16] Hanif MA, Nisar S, Rashid U. Supported solid and heteropoly acid catalysts for production of biodiesel. Cat Rev Sci Eng 2017;59:165–88.
[17] Alcañiz-Monge J, El Bakkali B, Trautwein G, Reinoso S. Zirconia-supported tungstophosphoric heteropolyacid as heterogeneous acid catalyst for biodiesel production. Appl Catal B Environ 2018;224:194–203.
[18] Furuta S, Matsuhashi H, Arata K. Biodiesel fuel production with solid superacid catalysis in fixed bed reactor under atmospheric pressure. Catal Commun 2004;5:721–3.
[19] López DE, Goodwin Jr JG, Bruce DA, Furuta S. Esterification and transesterification using modified-zirconia catalysts. Appl Catal A 2008;339:76–83.
[20] Istadi I, Anggoro DD, Buchori L, Rahmawati DA, Intaningrum D. Active acid catalyst of sulphated zinc oxide for transesterification of soybean oil with methanol to biodiesel. Procedia Environ Sci 2015;23:385–93.
[21] Mansir N, Taufiq-Yap YH, Rashid U, Lokman IM. Investigation of heterogeneous solid acid catalyst performance on low grade feedstocks for biodiesel production: a review. Energy Convers Manag 2017;141:171–82.
[22] Endalew AK, Kiros Y, Zanzi R. Heterogeneous catalysis for biodiesel production from Jatropha curcas oil (JCO). Energy 2011;36:2693–700.
[23] Di Serio M, Tesser R, Dimiccoli M, Cammarota F, Nastasi M, Santacesaria E. Synthesis of biodiesel via homogeneous Lewis acid catalyst. J Mol Catal A Chem 2005;239:111–5.
[24] Di Serio M, Carotenuto G, Cucciolito ME, Lega M, Ruffo F, Tesser R, Trifuoggi M. Shiff base complexes of zinc(II) as catalysts for biodiesel production. J Mol Catal A 2012;353(354):106–15.
[25] Barbosa SL, Dabdoub MJ, Hurtado GR, Klein SI, Baroni ACM, Cunha C. Solvent free esterification reactions using Lewis acids in solid phase catalysis. Appl Catal Gen 2006;313:146–50.
[26] Reinoso DM, Damiani DE, Tonetto GM. Zinc carboxylic salts used as catalyst in the Biodiesel synthesis by esterification and transesterificaction: study of the stability in the reaction medium. Appl Catal A 2012;449:88–95.
[27] Sousa SF, Fernandes PA, Ramos MJ. The carboxylate shift in zinc enzymes: a computational study. J Am Chem Soc 2007;129:1378–85.
[28] Aboelazayem O, El-Gendy NS, Abdel-Rehim AA, Ashour F, Sadek MA. Biodiesel production from castor oil in Egypt: process optimization, kinetic study, diesel engine performance and exhaust emissions analysis. Energy 2018;157:843–52.
[29] Krishnamurthy KN, Sridhara SN, Ananda Kumar CS. Synthesis and optimization of Hydnocarpus wightiana and dairy waste scum as feed stock for biodiesel production by using response surface methodology. Energy 2018;153:1073–86.
[30] Liu Y, Jiang Z, Li C. Emulsion catalysis: interface between homogeneous and heterogeneous catalysis. Bridging heterogeneous and homogeneous catalysis: concepts, strategies, and applications. John Wiley & Sons; 2014. p. 283–324.
[31] Naylor RL, Higgins MM. The political economy of biodiesel in an era of low oil prices. Renew Sustain Energy Rev 2017;77:695–705.
[32] Mahmudul HM, Hagos FY, Mamat R, Abdul Adam A, Ishak WFW, Alenezi R. Production, characterization and performance of biodiesel as an alternative fuel in diesel engines – a review. Renew Sustain Energy Rev 2017;72:497–509.
[33] Barman S, Vasudevan S. Contrasting melting behavior of zinc stearate and zinc oleate. J Phys Chem B 2006;110:651–4.
[34] Reinoso DM, Damiani DE, Tonetto GM. Efficient production of biodiesel from low-cost feedstock using zinc oleate as catalyst. Fuel Process Technol 2015;134:26–31.
[35] Santori G, Di Nicola G, Moglie M, Polonara F. A review analyzing the industrial biodiesel production practice starting from vegetable oil refining. Appl Energy 2012;92:109–32.
[36] Narváez PC, Noriega MA, Cadavid JG. Kinetics of palm oil ethanolysis. Energy 2015;83:337–42.
[37] release 2 gPROMS advanced user guide. 2004. p. 3.
[38] Li J, Zhang Y, Han D, Jia G, Gao J, Zhong L, Li C. Transfer hydrogenation of aldehydes on amphiphilic catalyst assembled at the interface of emulsion droplets. Green Chem 2008;10:608–11.
[39] Huang J, Yang H. A pH-switched pickering emulsion catalytic system: high reaction efficiency and facile catalyst recycling. Chem Commun 2015;51:7333–6.
[40] Gao JB, Zhang YN, Jia GQ, Jiang ZX, Wang SG, Lu HY, Song B, Li C. A direct imaging of amphiphilic catalysts assembled at the interface of emulsion droplets using fluorescence microscopy. Chem Commun 2008:332. 4.
[41] Slomkowski S, Alemán JV, Gilbert RG, Hess M, Horie K, Jones RG. Terminology of polymers and polymerization processes in dispersed systems (IUPAC Recommendations 2011). Pure Appl Chem 2011;83:2229–59.
[42] Li X, Zhang G, Dong J, Zhou X, Yan X, Luo M. Estimation of critical micelle concentration of anionic surfactants with QSPR approach. J Mol Struct: THEOCHEM 2004;710:119–26.
[43] Lucena IL, Canuto JDS, Caroni ALPF, Fonseca JLC, Dantas Neto AA, Castro Dantas TN. Characterization of nonionic surfactant micellar structures in organic solvents by small angle X-ray scattering (SAXS). Colloids Surf, A 2012;408:48–56.
[44] Ushikubo FY, Cunha RL. Stability mechanisms of liquid water-in-oil emulsions. Food Hydrocolloids 2014;34:145–53.
[45] Pugnet V, Maury S, Coupard V, Dandeu A, Quoineaud AA, Bonneau JL. Stability, activity and selectivity study of a zinc aluminate heterogeneous catalyst for the transesterification of vegetable oil in batch reactor. Appl Catal A 2010;374:71–8.
[46] Karmee SK, Chandna D, Ravi R, Chadha A. Kinetics of base-catalyzed transesterification of triglycerides from Pongamia oil. J Am Oil Chem Soc 2006;83:873–7.